

Simple Policy Gradients for Reasoning with Diffusion Language Models

Anthony Zhan¹

Abstract

Diffusion large language models (dLLMs), which offer a promising alternative to traditional autoregressive LLMs, have recently shown strong results in pretraining. However, due to their lack of tractable sequence-level likelihoods, they have yet to benefit from modern LLM post-training techniques such as reinforcement learning (RL), limiting their real-world applicability. Existing attempts at dLLM post-training rely on heuristic approximations or lower bounds of the true likelihood. In this work, we propose Amortized Group Relative Policy Optimization (AGRPO), a policy gradient algorithm that leverages the multi-step Markovian nature of dLLM generation, optimizing individual denoising steps rather than entire sequences. We demonstrate AGRPO’s effectiveness on different math and reasoning tasks, achieving +9.9% absolute gain on GSM8K, +4.6% on MATH-500, +59.4% on Countdown, and +69.7% on Sudoku over the base LLaDA model, improving upon comparable dLLM RL methods such as diffu-GRPO. Furthermore, we analyze how post-training gains persist across different inference configurations, revealing that models trained with AGRPO can sample 4x faster with minimal performance sacrifices.

1. Introduction

Many recent efforts in LLM research have centered around reinforcement learning, specifically in the verifiable reward (RLVR) setting. In a typical setup, base models are trained on math or coding problems and incentivized to reason through the solution step-by-step, getting a reward if the final answer is correct. The main goal of RLVR is to elicit mathematical thinking/reasoning capabilities, allowing models to solve complex real-world tasks.

This wave of interest in RL and reasoning, initially spurred by models like OpenAI’s o1 (OpenAI et al., 2024) and

DeepSeek’s R1 (DeepSeek-AI et al., 2025a), has led to the development of numerous post-training algorithms designed specifically for transformer-based autoregressive (AR) LLMs. With the success of these algorithms, chief among them Group Relative Policy Optimization (GRPO) (Shao et al., 2024), AR LLMs have grown incredibly strong on problem-solving benchmarks, with closed models even achieving gold medal performance at competitions such as the IMO and IOI, a remarkable feat (Luong & Lockhart, 2025; Lin & Cheng, 2025).

In a parallel line of research, diffusion language models have recently emerged as an alternative to the traditional autoregressive paradigm. Continuous diffusion models have long been established as the dominant framework for image and video generation, relying on a denoising/score matching objective. Works such as D3PM (Austin et al., 2021) and SEDD (Lou et al., 2024) successfully transferred this diffusion framework to discrete settings, including language. Successive efforts such as MDLM (Sahoo et al., 2024) and RADD (Ou et al., 2025) have simplified the theoretical framework, with most recent works settling on the “absorbing” or “masked” diffusion framework. We henceforth refer to this class of masked diffusion models as dLLMs.

Current state-of-the-art dLLMs, such as LLaDA (Nie et al., 2025) and MMaDA (Yang et al., 2025), are close to or on par with open-source AR models such as LLaMA3-8B and Qwen2.5-7B on common NLP benchmarks. Once trained, these models can go beyond standard left-to-right generation by starting with partially masked sequences, and additionally can trade off compute and quality by decreasing the number of sampling steps (i.e. sampling more tokens in parallel).

However, these models still struggle to match AR models in downstream tasks that require long-form thinking and reasoning. This discrepancy in post-training stems from fundamental challenges in designing training objectives for dLLMs: AR models have easy access to sequence-level likelihoods through AR factorization, whereas diffusion models must resort to approximations or ELBO-like bounds on likelihood. Unlocking true reasoning capabilities would be a giant leap forward for dLLMs, solidifying them as a true rival of AR LLMs.

Our work helps dLLMs close this gap by proposing a prin-

¹Stanford University. Correspondence to: Anthony Zhan <azhan9@stanford.edu>.

cipled policy gradient algorithm designed especially for dLLMs: Amortized Group Relative Policy Optimization (AGRPO). Unlike conventional one-step approaches, we first establish a multi-step MDP formulation of the post-training problem, tying it to the iterative unmasking process used by dLLMs. Then, through a simple modification of the policy gradient objective — by viewing the inner sum over all tokens as an expectation over timesteps — we show how to make training tractable for long-form reasoning tasks.

Our main contributions are as follows:

- **Soundness.** We derive an unbiased policy gradient objective from a multi-step view of the dLLM generation process, explaining how our approach sidesteps the need for heuristic likelihood approximations or ELBO-like bounds while remaining theoretically sound.
- **Efficiency.** Using statistical techniques, we show how to implement our proposed algorithm in a stable, memory-efficient way, and discuss various practical tradeoffs.
- **Efficacy.** We train models on four reasoning tasks (GSM8K, MATH, Countdown, and Sudoku), showing that AGRPO outperforms all previous approximation-based methods. In addition, we show that models post-trained with AGRPO retain high accuracy even when evaluated with much fewer sampling steps, a capability not found in pretrained base dLLMs.

2. Preliminaries

2.1. dLLM Pretraining

The most common form of discrete diffusion for language is the masked (or “absorbing”) approach, where models are trained to reverse data corrupted by randomly masking tokens (Lou et al., 2024; Sahoo et al., 2024; Arriola et al., 2025). Concretely, given a distribution p on sequences of discrete tokens $x = (x_1, \dots, x_n)$, models are trained to maximize the following evidence lower bound (ELBO) on the likelihood (Nie et al., 2025; Ou et al., 2025):

$$\mathcal{L}(\theta) = \mathbb{E}_{t \sim U[0,1]} \left[\frac{1}{t} \sum_{x_i^t = \blacksquare} \log p_\theta(x_i | x^t) \right] \quad (1)$$

where $x, x^t \sim p^t$ means that x is sampled from p and x^t is obtained from x by independently setting each token x_i to the mask token \blacksquare with probability t . Similar to BERT (Devlin et al., 2019), the goal is for the model to learn marginal distributions of masked tokens conditioned on context.

A crucial point is that compared to the classic AR objective, this masked token prediction objective is harder and

more general, since the unmasking order can be arbitrary and the model must predict *multiple* masked tokens. By contrast, AR models constrain themselves to modeling the *next* token in left-to-right order. The benefits of imposing this constraint are twofold: it lets AR models maximize the exact sequence likelihood via the chain rule, and it also lets training be parallelized via causal self-attention when used with decoder-only transformers.

2.2. dLLM Inference

To generate text, dLLMs start with an all- or partially-masked sequence, obtain marginal distributions for each masked token, and then unmask some of these by sampling from their marginals. The positions to be unmasked can be chosen either randomly, adhering to the theoretical “backward process,” or by keeping the tokens with highest probability, as proposed by Nie et al. (2025). (We refer to these as “random” and “confidence-based” unmasking, respectively.) The rest of the tokens are kept the same — masked tokens remain masked, unmasked tokens remain unmasked — and this new sequence is fed back into the model. This process is repeated until all tokens are unmasked.

Throughout this paper, we use m to refer to the number of sampling steps, and n to refer to the sequence length. A nice advantage of diffusion models is the ability to dynamically adjust the number of tokens unmasked per step n/m . Typically, the ratio n/m is chosen to be relatively small (≤ 8) — unmasking higher tokens at each step severely degrades quality as measured by perplexity or accuracy (Lou et al., 2024; Nie et al., 2025). We show in later sections that for specific tasks, post-training actually allows for much higher values of n/m without clear degradation, unlike pretrained models.

For more details on dLLM inference, see Appendix F.

2.3. Reinforcement Learning and MDPs

Markov decision processes (MDPs) are a formalization of sequential decision-making problems consisting of a state space \mathcal{S} , an action space \mathcal{A} , a transition kernel $p(\cdot | s, a)$, and a reward function $r(s, a)$. Broadly speaking, the goal of reinforcement learning (RL) is to learn a policy, i.e. a distribution $\pi(a | s)$, that maximizes the expected sum of rewards:

$$\mathbb{E}_{\tau \sim \pi} \left[\sum_{t=0}^T r(s_t, a_t) \right] \quad (2)$$

where τ represents a trajectory (or “rollout”), i.e. a sequence of states and actions $(s_0, a_0, s_1, a_1, \dots, s_T, a_T)$ where $a_i \sim \pi(\cdot | s_i)$ and $s_{i+1} \sim p(\cdot | s_i, a_i)$.

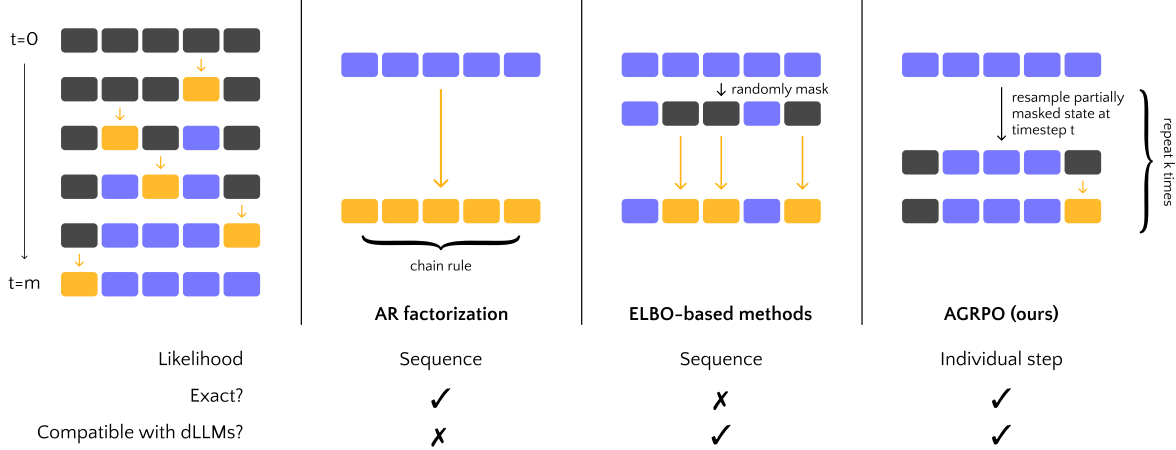


Figure 1. Existing RL post-training algorithms focus on sequence-level likelihoods and require either autoregressive factorization or ELBO-like bounds, which result in biased policy gradients. Our proposed algorithm instead focuses on individual unmasking steps, aligning more naturally with the dLLM generation process.

3. Policy Gradients for Diffusion Models

In this section, we describe our framing of dLLM post-training as a multi-step RL problem, which differs from the standard sequence-level framing of LLM post-training. To motivate this, we first give an overview of policy gradients.

3.1. Policy Gradient Methods

Policy gradients (PG) comprise a popular class of algorithms used to train neural network-parameterized policies π_θ to maximize expected rewards (Sutton et al., 1999). The simplest form of policy gradients, REINFORCE (Williams, 1992), involves the following gradient update:

$$\nabla_\theta \mathcal{J}_{PG}(\theta) = \mathbb{E}_{\tau \sim \pi} \left[\left(\sum_{t=0}^T \nabla_\theta \log \pi_\theta(a_t | s_t) \right) \left(\sum_{t=0}^T r(s_t, a_t) \right) \right]. \quad (3)$$

More sophisticated algorithms such as Proximal Policy Optimization (Schulman et al., 2017) improve upon this formulation by subtracting a learnable reward baseline (i.e. a value function) and allowing off-policy updates via an importance sampling correction. However, the underlying structure of all PG methods remains the same: compute the (exact) likelihoods of all actions along the trajectory, weighted by reward. Building on this common structure, we show how to develop a principled form of PG for dLLMs.

3.2. LLM Post-Training with RL

In the context of post-training LLMs, specifically RL with verifiable rewards (RLVR), the state s corresponds to the context (i.e. the prompt), actions a correspond to model outputs, and the reward r is provided via a ground truth answer. (Transitions are deterministic, so we can safely

ignore the transition kernel p .)

Thanks to AR factorization, one can view AR LLMs as policies that generate distributions over the entire sequence, i.e. a *one-step* MDP. Under this view, trajectories in (2) consist simply of the initial prompt s_0 and the model output a_0 . This makes the PG objective (3) quite convenient, and is quite effective for many post-training tasks; we discuss the large body of work devoted to this setting in Section 6.

3.3. Text Generation as a Multi-Step MDP

Diffusion models don't admit a clean left-to-right factorization, which makes sequence likelihoods intractable. In particular, for dLLMs such as LLaDA, computing the exact likelihood of a given length n sequence would require marginalizing over $O(n!)$ unmasking orders, which is simply infeasible for large n . Maximizing a lower bound on the likelihood suffices for pretraining, but is incompatible with the one-step MDP view of post-training, which requires exact sequence likelihoods.

While existing dLLM post-training approaches simply use an ELBO in place of the true likelihood, we would like to develop a more principled approach without such compromises. This motivates us to consider a *multi-step* MDP formulation of the generation process where

- the state s is the current partially masked sequence,
- the actions a are the n/m tokens to be unmasked¹, and
- the reward r is provided after the sequence is fully unmasked, i.e. at the last timestep.

¹The positions to be unmasked are determined by the unmasking strategy (random or confidence-based) and are not explicitly optimized, following theoretical assumptions of diffusion models.

In other words, a single step in this MDP is taken to be an individual unmasking step rather than the entire generation process.

This formulation, which aligns more naturally with how diffusion models are parameterized, has been adopted by previous works on RL for continuous diffusion such as DDPO and Flow-GRPO (Black et al., 2024; Liu et al., 2025a). Crucially, this perspective of denoising as a multi-step MDP allows for *exact action likelihoods* in the PG objective, sidestepping the need for lower bounds or approximations.

Remark 3.1. Treating dLLM generation as a multi-step MDP naturally aligns the partial masking states between inference and training, which is a key detail that one-step approaches often rely on (Wang et al., 2025a), but cannot theoretically justify.

3.4. Larger Models and Longer Trajectories

Note that although the multi-step perspective allows for exact likelihoods, computing (3) naively requires a separate forward pass for every denoising step. In domains such as robotics, the policy network and state representation are often small enough that one can batch many state-action pairs into a single forward pass.

However, for large diffusion models, particularly transformers which must attend to complex states, GPU memory significantly limits the potential for batching. (Using the batch dimension this way would also cut into the ability to batch multiple trajectories at once.) For image generation tasks where the number of steps m is smaller, spending m forward passes to compute the full objective can work, but this becomes impractical for reasoning tasks with hundreds of steps. We propose a novel way of addressing this problem via timestep sampling in Section 4.1.

4. Amortized Group Relative Policy Optimization

Before presenting the AGRPO objective, we first introduce some dLLM-specific notation. Let D be a distribution over questions q , $\{o^i\}_{i=1}^G$ a group of G outputs (or rollouts) conditioned on some q , and r_i the respective rewards. Each output has length n , and is generated with m unmasking steps. We use o_t to denote the partially masked state of rollout o at timestep t . For example, $\pi_\theta(o_1 | q, o_0)$ represents the probabilities of the first n/m tokens to be unmasked. (Recall that the unmasking order need not be left to right.)

4.1. From PPO to AGRPO

In this section, we show how to derive the AGRPO objective by reinterpreting the inner sum in the PG objective as an expectation across timesteps. Instead of the form given in

Equation (3), we work with PPO (Schulman et al., 2017), a more modern form which includes advantages and importance sampling (and clipping, which we temporarily omit for clarity). With the notation above, the PPO surrogate objective is:

$$\mathcal{J}(\theta) = \frac{1}{mG} \sum_{i=1}^G \sum_{t=1}^m \frac{\pi_\theta(o_t^i | q, o_{t-1}^i)}{\pi_{old}(o_t^i | q, o_{t-1}^i)} A_i \quad (4)$$

where $A_i = r_i - \text{mean}\{r_i\}$ is the advantage estimate and π_{old} is the policy under which rollouts are sampled, which is updated every μ gradient steps.

As in GRPO (Shao et al., 2024), we use group-normalized advantages for simplicity. Following subsequent improvements to GRPO, we avoid dividing by $\text{std}\{r_i\}$ to avoid bias from particularly easy or hard problems where advantages have low variance (Liu et al., 2025b).

Remark 4.1. Although the inner sum in (4) resembles the inner sum in the GRPO objective (Equation (3) in Shao et al. (2024)), we note that these are derived from fundamentally different assumptions: (4) arises from a sequential m -step unmasking process, whereas GRPO starts from a sequence-level objective and decomposes the importance sampling ratio into a sum of token-level ratios.

Now let T be a random variable drawn uniformly from $\{1, \dots, m\}$. Then an unbiased estimator of Equation (4) is

$$\frac{1}{G} \sum_{i=1}^G \mathbb{E}_{T \sim \{1, \dots, m\}} \left[\frac{\pi_\theta(o_T^i | q, o_{T-1}^i)}{\pi_{old}(o_T^i | q, o_{T-1}^i)} A_i \right].$$

Thus, with Monte Carlo (MC) sampling, the objective can now be estimated by drawing $k \ll m$ timesteps, computing the unmasking likelihood ratios, and averaging. Since the likelihoods are now at the individual timestep level, the resulting gradient estimate is *unbiased*, unlike existing works which substitute ELBOs for sequence likelihoods.

The full AGRPO objective with clipping is

$$\mathcal{J}(\theta) = \mathbb{E}_{\substack{q \sim D \\ \{o^i\}_{i=1}^G \sim \pi_{old}(\cdot | q)}} \left[\frac{1}{G} \sum_{i=1}^G \mathbb{E}_{t \sim \{1, \dots, m\}} \left[\min(\rho_t^i A_i, \text{clip}(\rho_t^i, 1 - \varepsilon, 1 + \varepsilon) A_i) - \beta D_{KL} \right] \right], \quad (5)$$

where

$$\rho_t^i = \frac{\pi_\theta(o_t^i | q, o_{t-1}^i)}{\pi_{old}(o_t^i | q, o_{t-1}^i)}$$

is the importance sampling ratio² and D_{KL} is shorthand for $D_{KL}(\pi_\theta || \pi_{ref})$. Note that under our multi-step framing, the

²Recall that dLLM inference works by factorizing the joint probability of unmasking n/m tokens as the product of marginals.

KL term represents the divergence over the specific positions unmasked at step t , i.e. $\pi_\theta(\cdot \mid q, o_{t-1}^i)$. This means we can also estimate it via MC sampling without relying on sequence-level approximations. To estimate D_{KL} , we use Schulman (2020)'s unbiased k_3 estimator

$$D_{\text{KL}}(p \parallel q) = \mathbb{E}_{x \sim p} \left[\frac{q(x)}{p(x)} - \log \frac{q(x)}{p(x)} - 1 \right]$$

which is also used by the original GRPO paper (Shao et al., 2024).

Algorithm 1 provides an overview of our proposed algorithm. For practical considerations, including how to efficiently retrieve partially masked states o_t and compute gradients, see Appendix E.

Algorithm 1 Amortized Group Relative Policy Optimization (AGRPO)

Require: policy π_θ , # sampling steps m , # MC samples k

```

 $\pi_{\text{ref}} \leftarrow \pi_\theta$ 
while not converged do
     $\pi_{\text{old}} \leftarrow \pi_\theta$ 
    sample prompt  $q \sim D$ 
    sample rollouts  $\{o^i\}_{i=1}^G \sim \pi_{\text{old}}(\cdot \mid q)$ 
    compute advantages  $\{\hat{A}_i\}$ 
    for  $\ell = 1$  to  $\mu$  do
         $\hat{J} \leftarrow 0$  {stores the MC estimate}
        for  $j = 1$  to  $k$  do
            sample  $t \sim \{1, \dots, m\}$  uniformly
             $\rho_t^i \leftarrow \frac{\pi_\theta(o_t^i \mid q, o_{t-1}^i)}{\pi_{\text{old}}(o_t^i \mid q, o_{t-1}^i)}$ 
             $\hat{J} \leftarrow \hat{J} + \sum_{i=1}^G \left[ \min \left( \text{clip} \left( \rho_t^i, 1 - \varepsilon, 1 + \varepsilon \right) A_i, \rho_t^i A_i \right) - \beta D_{\text{KL}}(\pi_\theta \parallel \pi_{\text{ref}}) \right]$ 
        end for
        compute AGRPO estimate  $\mathcal{J}(\theta) = \frac{\hat{J}}{kG}$ 
        backpropagate loss and take gradient step w.r.t.  $\theta$ 
    end for
end while

```

4.2. Variance Reduction Techniques

For a fixed number of samples k , a naive MC sampling algorithm would draw k i.i.d. samples, compute the objective, and average the results. We would ideally like an estimator with minimal variance to ensure stable training. Here we describe two such ways of reducing variance, and empirically test their effects in Section 5.5. The full variance-reduced AGRPO estimator, with a proof of unbiasedness, can be found in Appendix A.

4.2.1. Low-Discrepancy Sampling

Instead of i.i.d. sampling, we can introduce correlation across samples so that they collectively “cover” a wide range of timesteps while ensuring that the marginal distribution for each sample is still uniform on $\{1, \dots, m\}$. This is known as low-discrepancy sampling, and is used in practice to lower training variance for both continuous and discrete diffusion models (Kingma et al., 2021; Sahoo et al., 2024; Zheng et al., 2025). We follow Zheng et al. (2025)'s discrete low-discrepancy sampler, which is detailed in Appendix D.

A desirable property of low-discrepancy sampling is that in the limit $k \rightarrow m$, we fully recreate the original GRPO objective. In other words, one can achieve higher fidelity by scaling the amount of compute. We investigate this tradeoff induced by k in Section 5.4.

4.2.2. Entropy Importance Sampling

The uniform measure on $\{1, \dots, m\}$ treats all timesteps equally, even though it is plausible that not all tokens contribute equally to the final solution. Inspired by Wang et al. (2025b), who found that a minority of high-entropy tokens were responsible for the majority of performance gains in RLVR, we propose an entropy-based importance sampling scheme.

Instead of drawing $T \sim \{1, \dots, m\}$ uniformly, we compute an entropy score e_t for each timestep t by summing the entropies of the unmasked tokens at t . Then we draw T such that $\Pr[T = t] \propto e_t$, compute the objective given T , and multiply by a correction term $\sum e_t / (m e_T)$. This ensures that the model receives updates from critical reasoning tokens while remaining unbiased.

5. Experiments

To empirically validate our proposed algorithm, we start from the open source base model LLaDA-8B-Instruct (Nie et al., 2025) and fine-tune models using AGRPO on four different reasoning tasks: GSM8K, MATH, Countdown, and Sudoku.

5.1. Datasets

GSM8K/MATH are standard problem-solving benchmarks consisting of 8.5k/12.5k math problems at the grade school/high school level, respectively (Cobbe et al., 2021; Hendrycks et al., 2021). Countdown is a popular math reasoning task where the model is given a list of 3-4 numbers and a target number; the goal is to combine the numbers using arithmetic operations ($+, -, \times, /$) and parentheses to get the target number (Pan et al., 2025). Sudoku is a planning task where the goal is to fill in a 4x4 grid of numbers according to uniqueness constraints.

Table 1. Accuracies for different RL post-training methods across different reasoning tasks and generation lengths. For all diffusion models, outputs of length n are generated with $m = n/2$ steps. Few-shot examples are denoted in parentheses, and the best accuracy for each task is **bolded**. Models trained with LoRA (rather than full fine-tuning) are denoted with \dagger .

Model (AR)	GSM8K		MATH	
Model \ Seq len	256	512	256	512
DeepSeekMath-Base 7B			64.2	36.2
CoT SFT			82.9	46.8
CoT SFT + GRPO			88.2	51.7
GSM8K (0)		MATH-500 (0)		Countdown (0)
Model \ Seq len		256	512	256
LLaDA-8B-Instruct	79.9	78.2	36.6	37.4
LLaDA 1.5	81.4	81.1	35.4	40.6
diffu-GRPO †	79.8	81.9	37.2	39.2
wd1 † wd	80.8	82.3	34.4	39.0
SPG †	86.1	84.5	40.0	41.8
AGRPO (ours) †	88.0	88.1	39.4	42.0
GSM8K (0)		MATH-500 (0)		Sudoku (3)
Model \ Seq len		256	512	256
AGRPO (ours) †	88.0	88.1	39.4	42.0
				79.7
				82.4
				95.2
				95.2

These four tasks form the common set of benchmarks for the growing literature on dLLM reasoning (Wang et al., 2025a; Zhao et al., 2025; Tang et al., 2025). For consistency, we use the Countdown and Sudoku splits provided in SPG’s codebase (Wang et al., 2025a). We use HuggingFace’s math-verify library for parsing GSM8K, MATH, and Countdown answers.

5.2. Experimental Setup

Following previous dLLM RL works, we use Low-Rank Adaptation (Hu et al., 2021) instead of full fine-tuning. We fix the response length at $n = 384$ and the number of steps at $m = 128$ to balance inference wall time and coherence, both of which are important for RLVR, and we use $k = 24$ MC samples. Notably, despite being trained on a single configuration, we observe that model performance generalizes to different output lengths and steps.

During training, we generate rollouts with temperature 0.6 and random remasking to inject stochasticity and incentivize exploration. Random remasking makes additional sense in the context of AGRPO since it allows rollouts with similar final sequences to have vastly different intermediate states, helping the model learn from diverse contexts.

Models are trained until convergence is observed (e.g. via the reward curve plateauing); we select checkpoints from the last 150 steps for testing and report the best accuracy among those checkpoints. For evaluation, we switch to confidence-based unmasking (which can be thought of as a form of annealing (Nie et al., 2025)) with temperature 0, keeping the same generation process as previous works. Other hyperparameters, including G and ε , can be found in Appendix B.1.

Remark 5.1. Although our algorithm includes a KL penalty,

we find empirically that setting $\beta > 0$ does not yield any measurable benefits (and incurs an additional forward pass per gradient step), consistent with other RLVR works.

5.3. Results

Strong reasoning improvements. We report accuracies on test splits in Table 1. For diffusion models, AGRPO achieves the highest accuracy across all but one task, comfortably beating the base LLaDA model and other dLLM post-training methods, including diffu-GRPO (Zhao et al., 2025), VRPO (Zhu et al., 2025), and SPG (Wang et al., 2025a). At sequence length $n = 512$, we improve upon the previous best-known results by +1.4% on GSM8K, +0.2% on MATH-500, +12.1% on Countdown, and +2.1% on Sudoku. Baseline comparisons are discussed in greater detail in Appendix B.2.

Our results suggest that tailoring towards the Markovian nature of the diffusion process is the right way to extend AR LLM reasoning abilities to dLLMs, dispensing with the need for unprincipled approximations or bounds.

Comparable gains to GRPO. Although performance on MATH still lags behind autoregressive models, we are able to achieve parity with DeepSeekMath-RL on GSM8K, a substantial improvement for dLLMs. Additionally, we observe increased performance deltas for AGRPO compared to GRPO (e.g. for GSM8K, GRPO results in +5.3%, whereas AGRPO results in +9.9% at $n = 512$).

5.3.1. INFERENCE TRADEOFFS

A key quality of dLLMs is their ability to trade off compute and quality at inference time. We examine how AGRPO affects the inference compute/quality frontier by evaluating

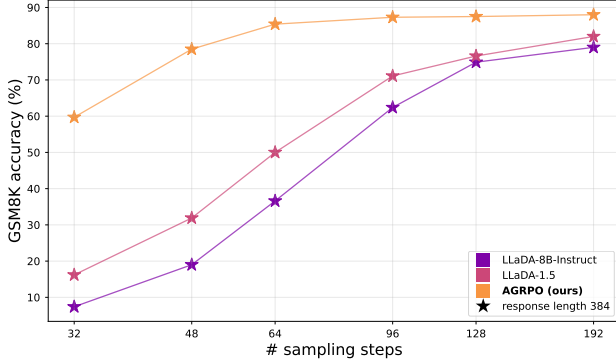


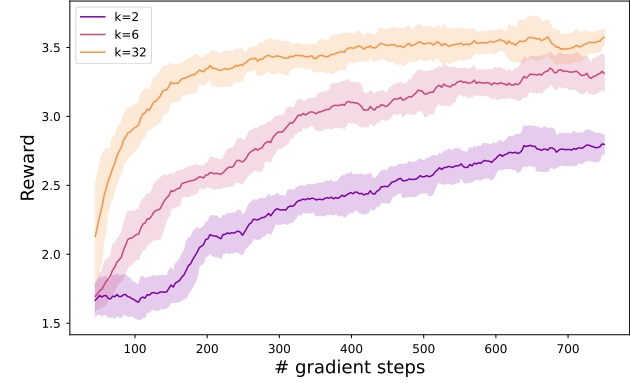
Figure 2. The compute/quality frontier for the GSM8K test split with response length $n = 384$. Lines show the possible tradeoffs at inference time for a specific model.

models on the GSM8K test split at a fixed response length $n = 384$ and varying the number of sampling steps m . As shown in Figure 2, not only does the AGRPO model consistently achieve higher performance across all sampling steps, it matches baselines with *4x fewer sampling steps*, a remarkable speedup. At the fastest setting, $m = 32$, AGRPO achieves 59.7% accuracy despite sampling 12 tokens per step, an 8.1x performance improvement over LLaDA-8B-Instruct and 3.7x improvement over LLaDA 1.5. These results demonstrate that the reasoning skills instilled by AGRPO are *robust*, generalizing to different inference configurations despite being trained on a fixed n and m . We give sample responses from this experiment in Appendix G.

To our knowledge, this is one of the first investigations of how post-training affects inference tradeoffs across a complete range of sampling steps, opening up a new perspective on the benefits of post-training dLLMs. As an example of a downstream application, model providers interested in a specific dLLM use case can pay a one-time fine-tuning cost in order to generate cheaper responses (i.e. low m) for that use case without sacrificing quality. In the long run, this amortization of inference costs could enable huge savings.

5.4. Ablations on k

With naive Monte Carlo sampling, increasing the number of samples by some factor c reduces the variance by c . This is the simplest lens through which to understand k , but the picture becomes slightly more nuanced in the context of online RL. For dLLMs, generating rollouts (which doesn't depend on k) is often more expensive than computing the actual policy update due to the large number of steps and lack of KV caching in dLLM inference. In other words, increasing k by 2x doesn't necessarily correspond to a 2x increase in overall training time. Thus, from an efficiency standpoint, choosing moderately large k is fine (as long as $k \ll m$).



(a) GSM8K reward over training runs with different k . The shaded area represents intra-run variance over a rolling window of 15 steps.

k	Average wall time (s)		
	Inference	Loss/backprop	Step
2	42.9	1.4	44.8
6	45.5	5.0	50.9
32	43.7	28.2	72.4

(b) Average wall time per gradient step for different components of AGRPO. Values are reported on 8xH100 GPUs with a global batch size of 128.

Figure 3. Reward curve and wall time comparisons for different values of k on GSM8K with $n = 384$ and $m = 128$.

As seen in Figure 3, our empirical findings are consistent with our expectations: larger values of k increase the wall time per step but converge faster. Note that although $k = 32$ spends almost 2x more compute per step than $k = 2$, it takes far more than 2x as many steps for $k = 2$ to reach the same reward level, suggesting that extremely small values of k are strictly worse.

To summarize, choosing k to be a healthy number relative to m (for example, $k \approx m/4$) is optimal not only because it improves the MC estimate, but because it helps “amortize” inference costs. Pinpointing the exact relationship between n , m , and the optimal value of k is an area we identify for future work.

For similar benchmarks against diffu-GRPO and SPG, see Appendix B.1.

5.5. Ablations on Variance Reduction Techniques

In this section, we investigate whether the variance reduction techniques proposed in Section 4.2 truly help empirically. We train two models, one with low-discrepancy sampling and entropy importance sampling and one without, on the Countdown task. All other hyperparameters, including the sequence length $n = 128$ and sampling steps $m = 64$, are the same between the two runs.

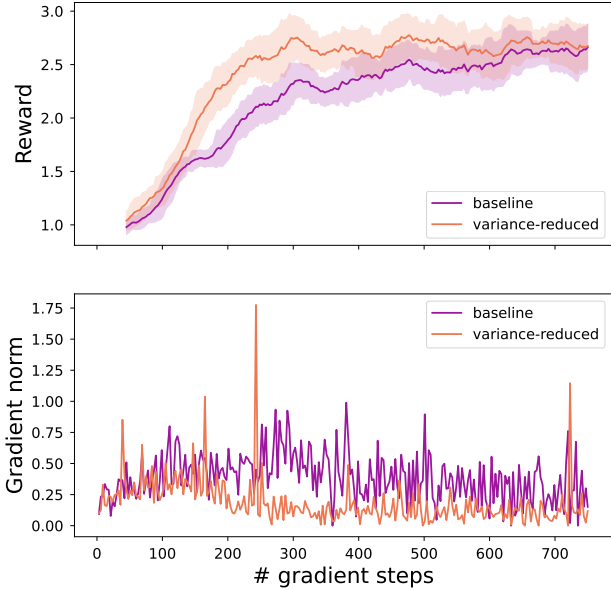


Figure 4. Reward and gradient norm plots for baseline and variance-reduced versions of AGRPO on Countdown with $n = 128$ and $m = 64$. The shaded area of the reward plot represents a rolling standard deviation with a window of 15 steps.

The reward curves and gradient norms are shown in Figure 4. Although both models reach a similar final reward level, the variance-reduced model converges faster, with less signs of early instability. In addition, the gradient norms for the variance-reduced model are consistently lower than the baseline throughout training (except for a few outlier steps). These results suggest that low discrepancy sampling and entropy-based importance sampling do indeed provide less noisy, more valuable updates.

6. Related Works

Policy gradient methods for LLMs. Early attempts at RL with LLMs (Ouyang et al., 2022; Ziegler et al., 2020) focused on alignment with human preferences using manually-labeled preference data and methods such as PPO or Direct Preference Optimization (Rafailov et al., 2023). More recently, RL efforts have focused on reasoning capabilities, specifically for domains with verifiable rewards such as math and coding. LLMs post-trained with algorithms such as GRPO exhibited improved reasoning abilities beyond SFT (Luo et al., 2025) and even emergent capabilities such as backtracking and self-correction (Xiong et al., 2025). Subsequent works modify GPRO to address issues in response length bias, sample efficiency, and stability (Yu et al., 2025; DeepSeek-AI et al., 2025b).

RL for continuous diffusion. Continuous diffusion models are highly popular in areas like image generation (Sohl-Dickstein et al., 2015; Peebles & Xie, 2022), video genera-

tion (Ho et al., 2022), and robotic control (Chi et al., 2024). To better align these models with desired downstream behavior, e.g. text-to-image tasks, different PG methods for diffusion have been proposed, including DDPO (Black et al., 2024) and DPPO (Ren et al., 2024). Crucially, these approaches formulate the RL problem as a multi-step denoising MDP, which our work extends to the dLLM setting for the first time.

RL for dLLM reasoning. Discrete diffusion models extend the diffusion framework to areas such as text and DNA sequences (Lou et al., 2024; Austin et al., 2021). As with traditional LLMs, there are many reasons to post-train dLLMs, including to elicit advanced reasoning capabilities. While some works focus on the more general continuous time/score entropy perspective (Zekri & Boullé, 2025), many works choose to focus on masked diffusion models such as LLaDA, which are more similar to traditional LLMs. Zhao et al. (2025) introduced the first dLLM post-training framework, d1, involving a CoT SFT stage followed by RLVR. Their proposed RL algorithm, diffu-GRPO, uses a mean-field approximation of the sequence likelihood along with random prompt masking. More recent works, such as wd1 (Tang et al., 2025) and SPG (Wang et al., 2025a), use more sophisticated ELBO-like bounds to achieve better empirical results. We discuss these works and others in more detail in Appendix C.

These methods, which assume the standard sequence-level framing of LLM post-training, rely on one-step likelihood approximations in order to remain tractable for dLLMs, thereby resulting in biased policy updates. We demonstrate that with the right diffusion-specific framing of RL — and some statistical techniques to make it practical — such approximations aren’t necessary to elicit strong reasoning skills.

7. Conclusion

This work presents AGRPO, a policy gradient algorithm designed for dLLMs, grounded in the multi-step denoising perspective of RL. Unlike previous dLLM RL works that rely on likelihood approximations or bounds, AGRPO computes policy gradient estimates in an unbiased, efficient way via Monte Carlo sampling and statistical variance reduction techniques, making it both principled and tractable. Using our proposed algorithm, we show how to effectively post-train dLLMs, beating comparable methods across multiple tasks and redefining the inference compute/quality frontier. These contributions establish AGRPO as a viable way to transfer policy gradient RL techniques to the dLLM setting; we hope future works can build on our methods, either theoretically or empirically, and further close the gap between dLLM and AR LLM post-training.

Impact Statement

This paper presents work whose goal is to advance the field of Machine Learning. There are many potential societal consequences of our work, none which we feel must be specifically highlighted here.

References

Arriola, M., Sahoo, S. S., Gokaslan, A., Yang, Z., Qi, Z., Han, J., Chiu, J. T., and Kuleshov, V. Block diffusion: Interpolating between autoregressive and diffusion language models. In *The Thirteenth International Conference on Learning Representations*, 2025. URL <https://openreview.net/forum?id=tyEyYT267x>.

Austin, J., Johnson, D. D., Ho, J., Tarlow, D., and van den Berg, R. Structured denoising diffusion models in discrete state-spaces. In Beygelzimer, A., Dauphin, Y., Liang, P., and Vaughan, J. W. (eds.), *Advances in Neural Information Processing Systems*, 2021. URL <https://openreview.net/forum?id=h7-XixPCAL>.

Black, K., Janner, M., Du, Y., Kostrikov, I., and Levine, S. Training diffusion models with reinforcement learning. In *The Twelfth International Conference on Learning Representations*, 2024. URL <https://openreview.net/forum?id=YCWjhGrJFD>.

Chi, C., Xu, Z., Feng, S., Cousineau, E., Du, Y., Burchfiel, B., Tedrake, R., and Song, S. Diffusion policy: Visuomotor policy learning via action diffusion, 2024. URL <https://arxiv.org/abs/2303.04137>.

Cobbe, K., Kosaraju, V., Bavarian, M., Chen, M., Jun, H., Kaiser, L., Plappert, M., Tworek, J., Hilton, J., Nakano, R., Hesse, C., and Schulman, J. Training verifiers to solve math word problems. *arXiv preprint arXiv:2110.14168*, 2021.

DeepSeek-AI, Guo, D., Yang, D., Zhang, H., Song, J., Zhang, R., Xu, R., Zhu, Q., Ma, S., Wang, P., Bi, X., Zhang, X., Yu, X., Wu, Y., Wu, Z. F., Gou, Z., Shao, Z., Li, Z., Gao, Z., Liu, A., Xue, B., Wang, B., Wu, B., Feng, B., Lu, C., Zhao, C., Deng, C., Zhang, C., Ruan, C., Dai, D., Chen, D., Ji, D., Li, E., Lin, F., Dai, F., Luo, F., Hao, G., Chen, G., Li, G., Zhang, H., Bao, H., Xu, H., Wang, H., Ding, H., Xin, H., Gao, H., Qu, H., Li, H., Guo, J., Li, J., Wang, J., Chen, J., Yuan, J., Qiu, J., Li, J., Cai, J. L., Ni, J., Liang, J., Chen, J., Dong, K., Hu, K., Gao, K., Guan, K., Huang, K., Yu, K., Wang, L., Zhang, L., Zhao, L., Wang, L., Zhang, L., Xu, L., Xia, L., Zhang, M., Zhang, M., Tang, M., Li, M., Wang, M., Li, M., Tian, N., Huang, P., Zhang, P., Wang, Q., Chen, Q., Du, Q., Ge, R., Zhang, R., Pan, R., Wang, R., Chen, R. J., Jin, R. L., Chen, R., Lu, S., Zhou, S., Chen, S., Ye, S., Wang, S., Yu, S., Zhou, S., Pan, S., Li, S. S., Zhou, S., Wu, S., Ye, S., Yun, T., Pei, T., Sun, T., Wang, T., Zeng, W., Zhao, W., Liu, W., Liang, W., Gao, W., Yu, W., Zhang, W., Xiao, W. L., An, W., Liu, X., Wang, X., Chen, X., Nie, X., Cheng, X., Liu, X., Xie, X., Liu, X., Yang, X., Li, X., Su, X., Lin, X., Li, X. Q., Jin, X., Shen, X., Chen, X., Sun, X., Wang, X., Song, X., Zhou, X., Wang, X., Shan, X., Li, Y. K., Wang, Y. Q., Wei, Y. X., Zhang, Y., Xu, Y., Li, Y., Zhao, Y., Sun, Y., Wang, Y., Yu, Y., Zhang, Y., Shi, Y., Xiong, Y., He, Y., Piao, Y., Wang, Y., Tan, Y., Ma, Y., Liu, Y., Guo, Y., Ou, Y., Wang, Y., Gong, Y., Zou, Y., He, Y., Xiong, Y., Luo, Y., You, Y., Liu, Y., Zhou, Y., Zhu, Y. X., Xu, Y., Huang, Y., Li, Y., Zheng, Y., Zhu, Y., Ma, Y., Tang, Y., Zha, Y., Yan, Y., Ren, Z. Z., Ren, Z., Sha, Z., Fu, Z., Xu, Z., Xie, Z., Zhang, Z., Hao, Z., Ma, Z., Yan, Z., Wu, Z., Gu, Z., Zhu, Z., Liu, Z., Li, Z., Xie, Z., Song, Z., Pan, Z., Huang, Z., Xu, Z., Zhang, Z., and Zhang, Z. Deepseek-r1: Incentivizing reasoning capability in llms via reinforcement learning, 2025a. URL <https://arxiv.org/abs/2501.12948>.

DeepSeek-AI, Liu, A., Mei, A., Lin, B., Xue, B., Wang, B., Xu, B., Wu, B., Zhang, B., Lin, C., Dong, C., Lu, C., Zhao, C., Deng, C., Xu, C., Ruan, C., Dai, D., Guo, D., Yang, D., Chen, D., Li, E., Zhou, F., Lin, F., Dai, F., Hao, G., Chen, G., Li, G., Zhang, H., Xu, H., Li, H., Liang, H., Wei, H., Zhang, H., Luo, H., Ji, H., Ding, H., Tang, H., Cao, H., Gao, H., Qu, H., Zeng, H., Huang, J., Li, J., Xu, J., Hu, J., Chen, J., Xiang, J., Yuan, J., Cheng, J., Zhu, J., Ran, J., Jiang, J., Qiu, J., Li, J., Song, J., Dong, K., Gao, K., Guan, K., Huang, K., Zhou, K., Huang, K., Yu, K., Wang, L., Zhang, L., Wang, L., Zhao, L., Yin, L., Guo, L., Luo, L., Ma, L., Wang, L., Zhang, L., Di, M. S., Xu, M. Y., Zhang, M., Zhang, M., Tang, M., Zhou, M., Huang, P., Cong, P., Wang, P., Wang, Q., Zhu, Q., Li, Q., Chen, Q., Du, Q., Xu, R., Ge, R., Zhang, R., Pan, R., Wang, R., Yin, R., Xu, R., Shen, R., Zhang, R., Liu, S. H., Lu, S., Zhou, S., Chen, S., Cai, S., Chen, S., Hu, S., Liu, S., Hu, S., Ma, S., Wang, S., Yu, S., Zhou, S., Pan, S., Zhou, S., Ni, T., Yun, T., Pei, T., Ye, T., Yue, T., Zeng, W., Liu, W., Liang, W., Pang, W., Luo, W., Gao, W., Zhang, W., Gao, X., Wang, X., Bi, X., Liu, X., Wang, X., Chen, X., Zhang, X., Nie, X., Cheng, X., Liu, X., Xie, X., Liu, X., Yu, X., Li, X., Yang, X., Li, X., Chen, X., Su, X., Pan, X., Lin, X., Fu, X., Wang, Y. Q., Zhang, Y., Xu, Y., Ma, Y., Li, Y., Li, Y., Zhao, Y., Sun, Y., Wang, Y., Qian, Y., Yu, Y., Zhang, Y., Ding, Y., Shi, Y., Xiong, Y., He, Y., Zhou, Y., Zhong, Y., Piao, Y., Wang, Y., Chen, Y., Tan, Y., Wei, Y., Ma, Y., Liu, Y., Yang, Y., Guo, Y., Wu, Y., Wu, Y., Cheng, Y., Ou, Y., Xu, Y., Wang, Y., Gong, Y., Wu, Y., Zou, Y., Li, Y., Xiong, Y., Luo, Y., You, Y., Liu, Y., Zhou, Y., Wu, Z. F., Ren, Z. Z., Zhao, Z., Ren, Z., Sha, Z., Fu, Z., Xu, Z., Xie, Z., Zhang, Z., Hao, Z., Gou, Z., Ma, Z., Yan, Z., Shao, Z., Huang, Z., Wu, Z.,

Li, Z., Zhang, Z., Xu, Z., Wang, Z., Gu, Z., Zhu, Z., Li, Z., Zhang, Z., Xie, Z., Gao, Z., Pan, Z., Yao, Z., Feng, B., Li, H., Cai, J. L., Ni, J., Xu, L., Li, M., Tian, N., Chen, R. J., Jin, R. L., Li, S. S., Zhou, S., Sun, T., Li, X. Q., Jin, X., Shen, X., Chen, X., Song, X., Zhou, X., Zhu, Y. X., Huang, Y., Li, Y., Zheng, Y., Zhu, Y., Ma, Y., Huang, Z., Xu, Z., Zhang, Z., Ji, D., Liang, J., Guo, J., Chen, J., Xia, L., Wang, M., Li, M., Zhang, P., Chen, R., Sun, S., Wu, S., Ye, S., Wang, T., Xiao, W. L., An, W., Wang, X., Sun, X., Wang, X., Tang, Y., Zha, Y., Zhang, Z., Ju, Z., Zhang, Z., and Qu, Z. Deepseek-v3.2: Pushing the frontier of open large language models, 2025b. URL <https://arxiv.org/abs/2512.02556>.

Devlin, J., Chang, M.-W., Lee, K., and Toutanova, K. Bert: Pre-training of deep bidirectional transformers for language understanding, 2019. URL <https://arxiv.org/abs/1810.04805>.

Hendrycks, D., Burns, C., Kadavath, S., Arora, A., Basart, S., Tang, E., Song, D., and Steinhardt, J. Measuring mathematical problem solving with the math dataset. *NeurIPS*, 2021.

Ho, J., Salimans, T., Gritsenko, A., Chan, W., Norouzi, M., and Fleet, D. J. Video diffusion models, 2022. URL <https://arxiv.org/abs/2204.03458>.

Hu, E. J., Shen, Y., Wallis, P., Allen-Zhu, Z., Li, Y., Wang, S., Wang, L., and Chen, W. Lora: Low-rank adaptation of large language models, 2021. URL <https://arxiv.org/abs/2106.09685>.

Huang, Z., Chen, Z., Wang, Z., Li, T., and Qi, G.-J. Reinforcing the diffusion chain of lateral thought with diffusion language models, 2025. URL <https://arxiv.org/abs/2505.10446>.

Kingma, D., Salimans, T., Poole, B., and Ho, J. Variational diffusion models. In Ranzato, M., Beygelzimer, A., Dauphin, Y., Liang, P., and Vaughan, J. W. (eds.), *Advances in Neural Information Processing Systems*, volume 34, pp. 21696–21707. Curran Associates, Inc., 2021. URL https://proceedings.neurips.cc/paper_files/paper/2021/file/b578f2a52a0229873fefc2a4b06377fa-Paper.pdf.

Lin, H. M. and Cheng, H. Gemini achieves gold-level performance at the international collegiate programming contest world finals. <https://deepmind.google/discover/blog/gemini-achieves-gold-level-performance-at-the-international-collegiate-programming-contest-world-finals> September 2025. Accessed: February 3, 2026.

Liu, J., Liu, G., Liang, J., Li, Y., Liu, J., Wang, X., Wan, P., Zhang, D., and Ouyang, W. Flow-grpo: Training flow matching models via online rl, 2025a. URL <https://arxiv.org/abs/2505.05470>.

Liu, Z., Chen, C., Li, W., Qi, P., Pang, T., Du, C., Lee, W. S., and Lin, M. Understanding r1-zero-like training: A critical perspective, 2025b. URL <https://arxiv.org/abs/2503.20783>.

Lou, A., Meng, C., and Ermon, S. Discrete diffusion modeling by estimating the ratios of the data distribution. In Salakhutdinov, R., Kolter, Z., Heller, K., Weller, A., Oliver, N., Scarlett, J., and Berkenkamp, F. (eds.), *Proceedings of the 41st International Conference on Machine Learning*, volume 235 of *Proceedings of Machine Learning Research*, pp. 32819–32848. PMLR, 21–27 Jul 2024. URL <https://proceedings.mlr.press/v235/lou24a.html>.

Luo, H., Sun, Q., Xu, C., Zhao, P., Lou, J., Tao, C., Geng, X., Lin, Q., Chen, S., Tang, Y., and Zhang, D. Wizardmath: Empowering mathematical reasoning for large language models via reinforced evol-instruct, 2025. URL <https://arxiv.org/abs/2308.09583>.

Luong, T. and Lockhart, E. Advanced version of gemini with deep think officially achieves gold-medal standard at the international mathematical olympiad. <https://deepmind.google/discover/blog/advanced-version-of-gemini-with-deep-think-officially-achieves-gold-medal-standard-at-the-international-mathematical-olympiad> July 2025. Accessed: February 3, 2026.

Ma, X., Yu, R., Fang, G., and Wang, X. dkv-cache: The cache for diffusion language models, 2025. URL <https://arxiv.org/abs/2505.15781>.

Nie, S., Zhu, F., You, Z., Zhang, X., Ou, J., Hu, J., Zhou, J., Lin, Y., Wen, J.-R., and Li, C. Large language diffusion models, 2025. URL <https://arxiv.org/abs/2502.09992>.

OpenAI, :., Jaech, A., Kalai, A., Lerer, A., Richardson, A., El-Kishky, A., Low, A., Helyar, A., Madry, A., Beutel, A., Carney, A., Iftimie, A., Karpenko, A., Passos, A. T., Neitz, A., Prokofiev, A., Wei, A., Tam, A., Bennett, A., Kumar, A., Saraiva, A., Vallone, A., Duberstein, A., Kondrich, A., Mishchenko, A., Applebaum, A., Jiang, A., Nair, A., Zoph, B., Ghorbani, B., Rossen, B., Sokolowsky, B., Barak, B., McGrew, B., Minaiev, B., Hao, B., Baker, B., Houghton, B., McKinzie, B., Eastman, B., Lugaressi, C., Bassin, C., Hudson, C., Li, C. M., de Bourcy, C., Voss, C., Shen, C., Zhang, C., Koch, C., Orsinger, C., Hesse, C., Fischer, C., Chan, C., Roberts, D., Kappler, D., Levy, D., Selsam, D., Dohan, D., Farhi, D., Mely, D., Robinson, D., Tsipras, D., Li, D., Oprica, D., Freeman, E., Zhang, E., Wong, E., Proehl, E., Cheung, E., Mitchell, E., Wallace, E., Ritter, E., Mays, E., Wang, F., Such, F. P., Raso, F., Leoni, F., Tsimpourlas, F., Song, F., von Lohmann, F., and Sutskever, I. Gemini achieves gold-level performance at the international collegiate programming contest world finals. <https://deepmind.google/discover/blog/gemini-achieves-gold-level-performance-at-the-international-collegiate-programming-contest-world-finals> September 2025. Accessed: February 3, 2026.

F., Sulit, F., Salmon, G., Parascandolo, G., Chabot, G., Zhao, G., Brockman, G., Leclerc, G., Salman, H., Bao, H., Sheng, H., Andrin, H., Bagherinezhad, H., Ren, H., Lightman, H., Chung, H. W., Kivlichan, I., O’Connell, I., Osband, I., Gilaberte, I. C., Akkaya, I., Kostrikov, I., Sutskever, I., Kofman, I., Pachocki, J., Lennon, J., Wei, J., Harb, J., Twore, J., Feng, J., Yu, J., Weng, J., Tang, J., Yu, J., Candela, J. Q., Palermo, J., Parish, J., Heidecke, J., Hallman, J., Rizzo, J., Gordon, J., Uesato, J., Ward, J., Huizinga, J., Wang, J., Chen, K., Xiao, K., Singhal, K., Nguyen, K., Cobbe, K., Shi, K., Wood, K., Rimbach, K., Gu-Lemberg, K., Liu, K., Lu, K., Stone, K., Yu, K., Ahmad, L., Yang, L., Liu, L., Maksin, L., Ho, L., Fedus, L., Weng, L., Li, L., McCallum, L., Held, L., Kuhn, L., Kondraciuk, L., Kaiser, L., Metz, L., Boyd, M., Trebacz, M., Joglekar, M., Chen, M., Tintor, M., Meyer, M., Jones, M., Kaufer, M., Schwarzer, M., Shah, M., Yatbaz, M., Guan, M. Y., Xu, M., Yan, M., Glaese, M., Chen, M., Lampe, M., Malek, M., Wang, M., Fradin, M., McClay, M., Pavlov, M., Wang, M., Wang, M., Murati, M., Bavarian, M., Rohaninejad, M., McAleese, N., Chowdhury, N., Chowdhury, N., Ryder, N., Tezak, N., Brown, N., Nachum, O., Boiko, O., Murk, O., Watkins, O., Chao, P., Ashbourne, P., Izmailov, P., Zhokhov, P., Dias, R., Arora, R., Lin, R., Lopes, R. G., Gaon, R., Miyara, R., Leike, R., Hwang, R., Garg, R., Brown, R., James, R., Shu, R., Cheu, R., Greene, R., Jain, S., Altman, S., Toizer, S., Toyer, S., Miserendino, S., Agarwal, S., Hernandez, S., Baker, S., McKinney, S., Yan, S., Zhao, S., Hu, S., Santurkar, S., Chaudhuri, S. R., Zhang, S., Fu, S., Papay, S., Lin, S., Balaji, S., Sanjeev, S., Sidor, S., Broda, T., Clark, A., Wang, T., Gordon, T., Sanders, T., Patwardhan, T., Sottiaux, T., Degry, T., Dimson, T., Zheng, T., Garipov, T., Stasi, T., Bansal, T., Creech, T., Peterson, T., Eloundou, T., Qi, V., Kosaraju, V., Monaco, V., Pong, V., Fomenko, V., Zheng, W., Zhou, W., McCabe, W., Zaremba, W., Dubois, Y., Lu, Y., Chen, Y., Cha, Y., Bai, Y., He, Y., Zhang, Y., Wang, Y., Shao, Z., and Li, Z. Openai o1 system card, 2024. URL <https://arxiv.org/abs/2412.16720>.

Ou, J., Nie, S., Xue, K., Zhu, F., Sun, J., Li, Z., and Li, C. Your absorbing discrete diffusion secretly models the conditional distributions of clean data. In *The Thirteenth International Conference on Learning Representations*, 2025. URL <https://openreview.net/forum?id=sMyXP8Tnm>.

Ouyang, L., Wu, J., Jiang, X., Almeida, D., Wainwright, C., Mishkin, P., Zhang, C., Agarwal, S., Slama, K., Ray, A., Schulman, J., Hilton, J., Kelton, F., Miller, L., Simens, M., Askell, A., Welinder, P., Christiano, P. F., Leike, J., and Lowe, R. Training language models to follow instructions with human feedback. In Koyejo, S., Mohamed, S., Agarwal, A., Belgrave, D., Cho, K., and Oh, A. (eds.), *Advances in Neural Information Processing Systems*, volume 35, pp. 27730–27744. Curran Associates, Inc., 2022. URL https://proceedings.neurips.cc/paper_files/paper/2022/file/blefde53be364a73914f58805a001731-Paper-Conference.pdf.

Pan, J., Zhang, J., Wang, X., Yuan, L., Peng, H., and Suhr, A. Tinyzero. <https://github.com/Jiayi-Pan/TinyZero>, 2025. Accessed: 2025-01-24.

Peebles, W. and Xie, S. Scalable diffusion models with transformers. *arXiv preprint arXiv:2212.09748*, 2022.

Rafailov, R., Sharma, A., Mitchell, E., Manning, C. D., Ermon, S., and Finn, C. Direct preference optimization: Your language model is secretly a reward model. In Oh, A., Naumann, T., Globerson, A., Saenko, K., Hardt, M., and Levine, S. (eds.), *Advances in Neural Information Processing Systems*, volume 36, pp. 53728–53741. Curran Associates, Inc., 2023. URL https://proceedings.neurips.cc/paper_files/paper/2023/file/a85b405ed65c6477a4fe8302b5e06ce7-Paper-Conference.pdf.

Ren, A. Z., Lidard, J., Ankile, L. L., Simeonov, A., Agrawal, P., Majumdar, A., Burchfiel, B., Dai, H., and Simchowitz, M. Diffusion policy policy optimization, 2024. URL <https://arxiv.org/abs/2409.00588>.

Sahoo, S. S., Arriola, M., Schiff, Y., Gokaslan, A., Marroquin, E., Chiu, J. T., Rush, A., and Kuleshov, V. Simple and effective masked diffusion language models. In Globerson, A., Mackey, L., Belgrave, D., Fan, A., Paquet, U., Tomczak, J., and Zhang, C. (eds.), *Advances in Neural Information Processing Systems*, volume 37, pp. 130136–130184. Curran Associates, Inc., 2024. URL https://proceedings.neurips.cc/paper_files/paper/2024/file/eb0b13cc515724ab8015bc978fdde0ad-Paper-Conference.pdf.

Schulman, J. Approximating kl divergence. <http://joschu.net/blog/kl-approx.html>, 2020. Blog post.

Schulman, J., Wolski, F., Dhariwal, P., Radford, A., and Klimov, O. Proximal policy optimization algorithms, 2017. URL <https://arxiv.org/abs/1707.06347>.

Shao, Z., Wang, P., Zhu, Q., Xu, R., Song, J., Bi, X., Zhang, H., Zhang, M., Li, Y. K., Wu, Y., and Guo, D. Deepseekmath: Pushing the limits of mathematical reasoning in open language models, 2024. URL <https://arxiv.org/abs/2402.03300>.

Sohl-Dickstein, J., Weiss, E. A., Maheswaranathan, N., and Ganguli, S. Deep unsupervised learning using nonequilibrium thermodynamics, 2015. URL <https://arxiv.org/abs/1503.03585>.

Sutton, R. S., McAllester, D., Singh, S., and Mansour, Y. Policy gradient methods for reinforcement learning with function approximation. In Solla, S., Leen, T., and Müller, K. (eds.), *Advances in Neural Information Processing Systems*, volume 12. MIT Press, 1999. URL https://proceedings.neurips.cc/paper_files/paper/1999/file/464d828b85b0bed98e80ade0a5c43b0f-Paper.pdf.

Tang, X., Dolga, R., Yoon, S., and Bogunovic, I. wd1: Weighted policy optimization for reasoning in diffusion language models, 2025. URL <https://arxiv.org/abs/2507.08838>.

Vendrow, J., Vendrow, E., Beery, S., and Madry, A. Do large language model benchmarks test reliability?, 2025. URL <https://arxiv.org/abs/2502.03461>.

von Werra, L., Belkada, Y., Tunstall, L., Beeching, E., Thrush, T., Lambert, N., Huang, S., Rasul, K., and Gallouédec, Q. Trl: Transformer reinforcement learning. <https://github.com/huggingface/trl>, 2020.

Wang, C., Rashidinejad, P., Su, D., Jiang, S., Wang, S., Zhao, S., Zhou, C., Shen, S. Z., Chen, F., Jaakkola, T., Tian, Y., and Liu, B. Spg: Sandwiched policy gradient for masked diffusion language models. *arXiv preprint arXiv:2510.09541*, 2025a.

Wang, S., Yu, L., Gao, C., Zheng, C., Liu, S., Lu, R., Dang, K., Chen, X., Yang, J., Zhang, Z., Liu, Y., Yang, A., Zhao, A., Yue, Y., Song, S., Yu, B., Huang, G., and Lin, J. Beyond the 80/20 rule: High-entropy minority tokens drive effective reinforcement learning for llm reasoning, 2025b. URL <https://arxiv.org/abs/2506.01939>.

Williams, R. J. Simple statistical gradient-following algorithms for connectionist reinforcement learning. *Machine Learning*, 8(3):229–256, 1992. doi: 10.1007/BF00992696. URL <https://doi.org/10.1007/BF00992696>.

Wu, C., Zhang, H., Xue, S., Liu, Z., Diao, S., Zhu, L., Luo, P., Han, S., and Xie, E. Fast-dllm: Training-free acceleration of diffusion llm by enabling kv cache and parallel decoding, 2025. URL <https://arxiv.org/abs/2505.22618>.

Xiong, W., Yao, J., Xu, Y., Pang, B., Wang, L., Sahoo, D., Li, J., Jiang, N., Zhang, T., Xiong, C., and Dong, H.

A minimalist approach to llm reasoning: from rejection sampling to reinforce, 2025. URL <https://arxiv.org/abs/2504.11343>.

Yang, L., Tian, Y., Li, B., Zhang, X., Shen, K., Tong, Y., and Wang, M. Mmada: Multimodal large diffusion language models, 2025. URL <https://arxiv.org/abs/2505.15809>.

Yao, F., Liu, L., Zhang, D., Dong, C., Shang, J., and Gao, J. Your efficient rl framework secretly brings you off-policy rl training, August 2025. URL <https://fengyao.notion.site/off-policy-rl>.

Yu, Q., Zhang, Z., Zhu, R., Yuan, Y., Zuo, X., Yue, Y., Dai, W., Fan, T., Liu, G., Liu, L., Liu, X., Lin, H., Lin, Z., Ma, B., Sheng, G., Tong, Y., Zhang, C., Zhang, M., Zhang, W., Zhu, H., Zhu, J., Chen, J., Chen, J., Wang, C., Yu, H., Song, Y., Wei, X., Zhou, H., Liu, J., Ma, W.-Y., Zhang, Y.-Q., Yan, L., Qiao, M., Wu, Y., and Wang, M. Dapo: An open-source llm reinforcement learning system at scale, 2025. URL <https://arxiv.org/abs/2503.14476>.

Zekri, O. and Boullé, N. Fine-tuning discrete diffusion models with policy gradient methods, 2025. URL <https://arxiv.org/abs/2502.01384>.

Zhao, S., Gupta, D., Zheng, Q., and Grover, A. d1: Scaling reasoning in diffusion large language models via reinforcement learning, 2025. URL <https://arxiv.org/abs/2504.12216>.

Zheng, K., Chen, Y., Mao, H., Liu, M.-Y., Zhu, J., and Zhang, Q. Masked diffusion models are secretly time-agnostic masked models and exploit inaccurate categorical sampling. In *The Thirteenth International Conference on Learning Representations*, 2025. URL <https://openreview.net/forum?id=CTC7CmirNr>.

Zhu, F., Wang, R., Nie, S., Zhang, X., Wu, C., Hu, J., Zhou, J., Chen, J., Lin, Y., Wen, J.-R., and Li, C. Llada 1.5: Variance-reduced preference optimization for large language diffusion models, 2025. URL <https://arxiv.org/abs/2505.19223>.

Ziegler, D. M., Stiennon, N., Wu, J., Brown, T. B., Radford, A., Amodei, D., Christiano, P., and Irving, G. Fine-tuning language models from human preferences, 2020. URL <https://arxiv.org/abs/1909.08593>.

A. Proof of Unbiased Estimator

Using the notation of Section 4.1, define the entropy score e_t as the Shannon entropy of $\pi(o_t \mid q, o_{t-1})$, i.e. the sum of the marginal entropies of the positions unmasked at step t . Let $\bar{e} = \{e_t / \sum e_t\}_{t=1}^m$ be the vector of normalized entropy scores, and suppose $T \sim \text{Cat}(\bar{e})$. Then the full AGRPO estimator (without clipping) is

$$\widehat{\mathcal{J}}(\theta; T) = \frac{1}{mG\bar{e}_T} \sum_{i=1}^G \frac{\pi_\theta(o_T^i \mid q, o_{T-1}^i)}{\pi_{old}(o_T^i \mid q, o_{T-1}^i)} A_i.$$

Theorem A.1. $\mathbb{E}[\widehat{\mathcal{J}}(\theta; T)] = \mathcal{J}(\theta)$, where $\mathcal{J}(\theta)$ is defined in Equation (4) and the expectation is taken w.r.t. randomness of T .

Proof. Since T is a categorical random variable, we can write out the expectation explicitly:

$$\begin{aligned} \mathbb{E}[\widehat{\mathcal{J}}(\theta)] &= \sum_{t=1}^m \Pr[T = t] \frac{1}{mG\bar{e}_t} \sum_{i=1}^G \frac{\pi_\theta(o_t^i \mid q, o_{t-1}^i)}{\pi_{old}(o_t^i \mid q, o_{t-1}^i)} A_i \\ &= \sum_{t=1}^m \frac{e_t}{\sum_{t'=1}^m e_{t'}} \frac{\sum_{t'=1}^m e_{t'}}{mG\bar{e}_t} \sum_{i=1}^G \frac{\pi_\theta(o_t^i \mid q, o_{t-1}^i)}{\pi_{old}(o_t^i \mid q, o_{t-1}^i)} A_i \\ &= \frac{1}{mG} \sum_{t=1}^m \sum_{i=1}^G \frac{\pi_\theta(o_t^i \mid q, o_{t-1}^i)}{\pi_{old}(o_t^i \mid q, o_{t-1}^i)} A_i = \mathcal{J}(\theta). \end{aligned}$$

□

Remark A.2. There are many potential unbiased ways to estimate the PG objective with Monte Carlo sampling; resampling timesteps is a natural way, but there could be other ways to optimally reduce variance and speed up training, e.g. different importance sampling schemes. We leave such explorations for future work.

B. Experiment Details

B.1. Training

Models are trained with LoRA rank $r = 64$ on 8xH100 GPUs for 400-900 steps (depending on the task). We use Hugging Face’s TRL framework (von Werra et al., 2020) to implement the training code. Rewards are a combination of rule-based formatting rewards, i.e. the presence of `<think>` and `<answer>` tags, as well as binary ground-truth rewards (except for Sudoku, where the reward is the fraction of empty cells filled in correctly, which is dense).

For batched rollouts, we use a group size of $G = 8$ per prompt and 16 prompts per update, resulting in a global batch size of 128. The clipping threshold is set to $\varepsilon = 0.2$. The number of gradient updates per batch of rollouts μ , which controls the “off-policyness” of the algorithm, is set to $\mu = 1$. As mentioned previously, we also assume $\beta = 0$, so the algorithm is fully on-policy with no KL penalty. Consistent with Yu et al. (2025) and Tang et al. (2025), we don’t observe any drawbacks in terms of convergence speed or stability with this configuration.

Since AGRPO involves multiple forward passes per gradient step, it incurs a higher wall-clock cost per update than one-step methods like diffu-GRPO and SPG (see Table 2). However, because AGRPO updates the policy based on a wide range of intermediate states rather than only the final sequence, it provides a denser learning signal and therefore improved sample efficiency (i.e. requires fewer rollouts). Empirically, we observe rapid convergence to high reward levels across all tasks (see e.g. Figures 3a and 4), suggesting that the additional compute per step is offset by higher quality gradient updates.

Remark B.1. As previously emphasized, the main bottleneck in online RL with dLLMs is the inference time. Thus the additional cost of AGRPO’s repeated sampling is not as drastic as one might think; the increase in FLOPs per step is commensurate with modest increases in context length or batch size, which are commonly used to trade compute for optimization stability.

Table 2. Average wall time per gradient step for different dLLM RL methods on a controlled GSM8K training run with $n = 256$, $m = 128$, $G = 4$, and $\mu = 2$. Values are reported on 2xRTX6000 Ada GPUs with a global batch size of 16.

Method	Average wall time (s)		
	Inference	Loss/backprop	Step
diffu-GRPO	42.4	0.5	43.8
SPG	41.9	1.0	44.6
AGRPO ($k = 8$)	41.6	10.4	53.3

B.2. Evaluation

For all tasks and train/test splits, we use open source datasets from HuggingFace or GitHub. Accuracies for GSM8K are reported on the GSM8K-Platinum (Vendrow et al., 2025) test split, a cleaned version of the original GSM8K test split. Surprisingly, we found that models trained on GSM8K problems achieved higher accuracy on MATH-500 test problems than models trained on the MATH training split. The accuracy reported in Table 1 is thus from the GSM8K model; models trained on MATH showed more modest gains, achieving 38.0% at $n = 256$. We hypothesize that the more difficult nature of MATH, combined with inherent limitations of the base LLaDA model and limited context window, make it harder to learn generalizable reasoning abilities during RL.

Results for diffu-GRPO, wd1, and SPG are taken from the respective papers (Zhao et al., 2025; Tang et al., 2025; Wang et al., 2025a). We note that our reproduced baselines for LLaDA-8B-Instruct and LLaDA 1.5 are slightly higher than baselines reported in the aforementioned works (and that there is variation between these works as well). We attribute this to our use of a more amenable system prompt and robust parsing system (via symbolic libraries), which we applied consistently across all tasks to ensure a fair comparison.

For completeness, we provide a full comparison of reported LLaDA-8B-Instruct baselines against Zhao et al. (2025) and Wang et al. (2025a) in Table 3.

Table 3. Comparison of base model accuracies reported in previous work vs. reproduced in our work.

Work	Model \ Seq len	GSM8K		MATH-500		Countdown		Sudoku	
		256	512	256	512	256	512	256	512
d1 (Zhao et al., 2025)	LLaDA-8B-Instruct	76.7	78.2	32.4	36.2	19.5	16.0	6.7	5.5
SPG (Wang et al., 2025a)	LLaDA-8B-Instruct	77.2	79.8	32.4	34.6	16.8	16.8	27.7	26.2
AGRPO (ours)	LLaDA-8B-Instruct	79.9	78.2	36.6	37.4	20.3	27.3	25.5	18.8

C. Comparisons to Previous dLLM Post-Training Methods

Here we continue our discussion of dLLM post-training methods presented in Section 6.

wd1. Tang et al. (2025) build on diffu-GRPO by leveraging the closed-form solution π^* of reverse KL-regularized policy optimization, namely $\pi^*(a | s) \propto \pi_{\text{ref}}(a | s) \exp(r(s, a) / \beta)$ where β is the reverse KL coefficient. They use this to rewrite the PG objective in way that simplifies the importance sampling ratio $\pi_\theta(\cdot | q) / \pi_{\text{old}}(\cdot | q)$. However, their approach inherits from d1 the same reliance on one-step approximations, limiting practical effectiveness.

VRPO. Introduced by Zhu et al. (2025) as part of the training process for LLaDA 1.5, Variance-Reduced Policy Optimization follows a similar approach to DPO (Rafailov et al., 2023), where the model directly learns from pairwise preference data without external rewards. The VRPO objective consists of the DPO objective with all sequence likelihoods replaced by ELBOs, along with several tricks to reduce variance. Overall, the LLaDA 1.5 paper studies a slightly different RL setting (alignment/RLHF instead of reasoning/RLVR) and also relies heavily on likelihood bounds.

DCoLT. Inspired by autoregressive chain-of-thought methods, Huang et al. (2025) optimize a Diffusion Chain of Lateral Thought. Similar to our approach, they adopt a multi-step denoising view where actions consists of individual unmasking steps rather than the final sequence. However, there are several key differences that make AGRPO training much simpler:

DCoLT requires training a separate module to rank which positions to unmask (according to a Plackett-Luce model) and accumulates gradients over *all m timesteps* instead of using MC sampling to estimate gradients efficiently.

SPG. Most recently, Wang et al. (2025a) propose Sandwiched Policy Gradients, which combines an ELBO-like lower bound on likelihood with an evidence upper bound (EUBO). They identify an issue with PG objectives that doesn’t appear in dLLM pretraining, namely the fact that likelihoods can be multiplied by a negative advantage estimate, which breaks the validity of optimizing a lower bound. By optimizing the EUBO in place of the standard ELBO for negative advantage trajectories, they achieve stronger empirical results (although their policy updates remain biased due to the sequence-level framing).

D. Low-discrepancy Sampling Details

An outline of Zheng et al. (2025)’s discrete low-discrepancy sampler is given below. The goal is draw k samples from $T \sim \{0, \dots, m-1\}$.

1. Sample U_0, \dots, U_{k-1} i.i.d. from $\text{Unif}([0, 1])$.
2. “Bin” them into k disjoint bins by defining $U'_j = (U_j + j)/k$ for $j = 0$ to $k-1$.
3. Define the final set of k samples $\{T_j\}_{j=0}^{k-1}$ as $T_j = \lfloor mU'_j \rfloor$.

Intuitively, the sampler divides the interval $[0, 1]$ into k equal subintervals, samples from each one uniformly and shuffles the results, and then scales by a factor of m and floors. In AGRPO, this allows us to “cover” a wide range of timesteps from 1 to m when estimating the PG objective. We can also extend this to the batch level: instead of sampling k timesteps, we sample bk timesteps where b is the batch size.

To use low-discrepancy sampling in conjunction with entropy importance sampling, we replace Step 3 by an inverse CDF transform to turn samples from $\text{Unif}([0, 1])$ into categorical samples.

E. Practical Considerations

In this section, we discuss in detail various decisions and tradeoffs made regarding the actual implementation of AGRPO. As with all online RL algorithms, the goal of any implementation is to run as efficiently as possible while maximizing efficacy. We plan to release training and evaluation code publicly to showcase implementation details and encourage reproducibility.

Caching partially masked states. In order to obtain exact action/token likelihoods, we must recreate the exact state/context at the step where that token was unmasked. To do this efficiently, we cache the unmasking order during generation so that each token is associated with a timestep t . Then, to get the partially masked state at timestep t , we simply mask out all tokens with timestep $\geq t$.

Memory-efficient gradient accumulation. Naively computing the AGRPO objective (5) and backpropagating would require keeping k forward passes simultaneously in memory, which can quickly saturate GPU memory for 8B scale models. Instead, one can accumulate the gradient immediately after each MC sample is computed by calling `loss.backward()` (without taking an optimizer step) *inside* the for loop. This frees the computational graph and avoids excess memory usage.

float64 Gumbel-based categorical sampling. dLLMs typically use the Gumbel-max trick to sample from output logits. However, Zheng et al. (2025) point out that naively using `float32` causes an inconsistency between theoretical and actual behavior due to floating-point precision. We follow their recommendation of using `float64` for the sampling stage.

Handling EOS tokens. Since dLLMs generate with a fixed number of sampling steps, in later timesteps, the model can spend many “garbage” steps producing EOS tokens at the end of a sequence (while other sequences in the batch are still generating useful tokens). Gradient updates on these steps don’t provide meaningful information to the model, so we set the max timestep in our low-discrepancy sampler (Section D) to be the last timestep where a non-EOS token was generated.

Training/inference mismatches. Yao et al. (2025) observe that for RL with traditional LLMs, mismatches between the inference engine and training code can cause subtle “off-policyness” and instability issues, especially when combined with `bf16` precision. For AGRPO, we deploy a custom inference engine for LLaDA, making sure to track things such as the top-p/top-k sampling masks and reuse them in training, as suggested by DeepSeek-AI et al. (2025b).

F. Remarks on dLLM Inference

Despite a more complicated training setup, dLLMs enjoy several potential benefits at inference time: they can generate text in arbitrary order, are naturally self-speculative (i.e. one can see the model’s best guess for the entire sequence at every step), and can trade off compute and generation quality by choosing to unmask more or less tokens per step.

Here we discuss several unique characteristics of dLLM inference, which may be helpful to readers who are only familiar with traditional AR LLM inference.

Fixed sequence length. One drawback of dLLMs is that the context length must be fixed ahead of time, instead of being dynamically grown as with AR LLMs. Works such as BlockDiff address this issue by introducing a hybrid autoregressive/diffusion framework (Arriola et al., 2025); in this paper, we stay within the normal diffusion framework for simplicity.

Instruct-tuned models. dLLMs such as LLaDA-8B-Instruct, which have undergone supervised fine-tuning (SFT) on instruction-following traces, tend to place higher probabilities on EOS tokens. When combined with confidence-based unmasking, this leads to an unnaturally high proportion of EOS tokens in later positions and terse, stilted responses (Nie et al., 2025). Thus, to generate text with standard left-to-right prompting, we divide the response into smaller blocks, unmask tokens within the leftmost block, and continue to the next block once all tokens in the current block have been unmasked. This is known as *semi-autoregressive* sampling (Yang et al., 2025). During training, we use semi-AR sampling with block length 12.

Bidirectional prompting. In this paper, we work with traditional left-to-right prompting, which is the native format for the reasoning datasets we use. This leaves a big dLLM advantage on the table — namely their ability to generate text from arbitrary context. Future works could consider reasoning tasks that involve using context from both the left and right; for example, giving the model a problem and the numerical answer, and forcing it to deduce the intermediate steps.

KV caching. Since diffusion transformers typically use full self-attention instead of causal self-attention (Peebles & Xie, 2022), embeddings for the same token position can change over the sampling process. This non-causality prevents dLLMs from using the same KV caching mechanism as AR LLMs. As a result, generating same-quality text with dLLMs is significantly slower than same-scale AR models, which is especially painful for online RL. However, there has been some recent interest in KV caching alternatives for dLLMs (Wu et al., 2025; Ma et al., 2025). Since dLLMs already have the ability to decode multiple tokens in parallel, we believe a successful implementation of KV caching is imperative to realizing dLLMs’ potential as a faster, more flexible alternative to AR models.

G. Sample Responses

See Table 4 for the system prompt used in GSM8K training as well as sample responses from a chosen test split problem. As evident in the responses, RL induces a rigid step-by-step structure, which we hypothesize allows the model to arrive at the same solution with many less steps ($m = 48$ vs $m = 192$). could explain the results in Section 5.3.1

Even though both responses arrive at the correct answer, the $m = 192$ solution is more coherent, while the $m = 48$ solution contains clear artifacts (i.e. repeated words, grammar mistakes). Note that the model is only trained on $m = 128$, so such artifacts are technically out-of-distribution and could ostensibly “derail” the model. Our results show the contrary, however, suggesting that learned reasoning abilities are robust to such perturbations.

Remark G.1. Overall, we observe that models trained with AGRPO can exhibit signs of entropy collapse, namely reduced token diversity and formulaic, “template”-y answers. This is consistent with findings in the broader RLVR literature, and could also be explained by the task-specific training process. Future works could explore ways to mitigate entropy collapse by e.g. setting a higher clipping threshold in the clipped objective (Yu et al., 2025).

Table 4. Sample responses ($n = 384$) for different values of m (# sampling steps) from a model trained with AGRPO. Problem is from the GSM8K-Platinum dataset.

System:

```
You will be given a math problem.
Think through the problem step by step, enclosing your reasoning process
in <think> tags.
Provide your final answer in <answer> tags, with only the number or
expression enclosed in \boxed{}, as follows:
<think>
...
</think>
<answer>
\boxed{...}
</answer>
```

User:

Tommy is fundraising for his charity by selling brownies for \$3 a slice and cheesecakes for \$4 a slice. If Tommy sells 43 brownies and 23 slices of cheesecake, how much money does Tommy raise?

Assistant (m=48):

```
<think>
First, we need to calculate the total from selling brownies.
Each brownie is $3 and Tommy sells 43 brownies
\[
3 \times 43 = 129
\]
Next, we calculate the total from selling cheesecakes.
Each slice of cheesecake is $4 and sells 23 slices is:
\[
4 \times 23 = 92
\]
Finally, we add these two amounts to find the total money raised by
Tommy:
\[
129 + 92 = 221
\]
</think>
<answer>
\boxed{221}
</answer>
```

Assistant (m=192):

```
<think>
First, we need calculate the money raised from selling the brownies.
Tommy sells 43 brownies at $3 each:
\[
43 \times 3 = 129
\]
Next, we calculate the money raised from selling the cheesecakes. Tommy
sells 23 slices of cheesecake at $4 each:
\[
23 \times 4 = 92
\]
Finally, we add these two amounts together to find the total amount of
money raised:
\[
129 + 92 = 221
\]
</think>
<answer>
\boxed{221}
</answer>
```